*nanomaterials*

MDPI

*Review*

# Doped Carbon Dots for Sensing and Bioimaging Applications: A Minireview

**Timur Sh. Atabaev**

Department of Chemistry, School of Science and Technology, Nazarbayev University, Astana 010000, Kazakhstan; timuratabaev@yahoo.com or timur.atabaev@nu.edu.kz

Received: 3 May 2018; Accepted: 15 May 2018; Published: 18 May 2018


**Abstract:** In the last decade, carbon dots (C-dots, CDs) or carbon quantum dots (CQDs) have attracted a considerable amount of attention from the scientific community as a low cost and biocompatible alternative to semiconductor quantum dots. In particular, doped C-dots have excellent fluorescent properties that have been successfully utilized for numerous applications. In this minireview, we overview the recent advances on the synthesis of doped C-dots derived from carbon-rich sources and their potential applications for biomedical and sensing applications. In addition, we will also discuss some challenges and outline some future perspectives of this exciting material.

**Keywords:** carbon dots; doping; fluorescent propertum dots with pH- and thies; sensing; bioimaging

## 1. Introduction

Carbon dots were first discovered in 2004 during single-walled carbon nanotubes purification [1]. These C-dots can be described as quasi-spherical particles with sizes below 10 nm. Figure 1 shows that the number of scientific publications related to C-dots rapidly raised starting from 2005. The increased interest in these materials is related to several advantages of C-dots, such as carbon source abundance, simple and low-cost synthesis process, biocompatibility, and excellent fluorescent properties. In addition, C-dots are chemically stable, inert, form a stable colloidal solution, and are highly resistant to photobleaching compared to traditional fluorescent organic dyes and semiconductor quantum dots. Therefore, the fluorescent properties of C-dots are widely utilized for sensing [2–4], biomedical imaging [5–7], catalysis [8,9], energy research [10,11], etc. A number of review articles related to the synthesis and various applications of C-dots were published recently [1,4,11]. On the other hand, a focused overview of doped C-dots for potential biomedical and sensing applications is still not available in the literature. Therefore, in this minireview, we briefly discuss the synthesis and fluorescent properties of doped C-dots obtained from carbon-rich sources. Next, we review recent representative works related to the sensing and biomedical applications of doped C-dots. Finally, we will provide some future perspectives and highlight the importance of doping strategy for the development of advanced multifunctional nanoprobes.

## 2. Synthesis and Optical Properties of Doped C-Dots

Various synthetic methods such as chemical etching [12], electrochemical carbonization [13], laser ablation [14], microwave irradiation [15], and hydrothermal/solvothermal [16,17] methods have been widely employed for the preparation of fluorescent C-dots. Considering the enormous potential of C-dots for numerous applications, it is extremely necessary to develop their large-scale synthesis. From this point of view, the hydrothermal synthesis has become the most popular method due to its simplicity, low-cost, and high efficiency. In this method, one should simply heat the water and carbon-rich compounds (sugars, organic molecules) in a tightly closed vessel to initiate the carbonization process.

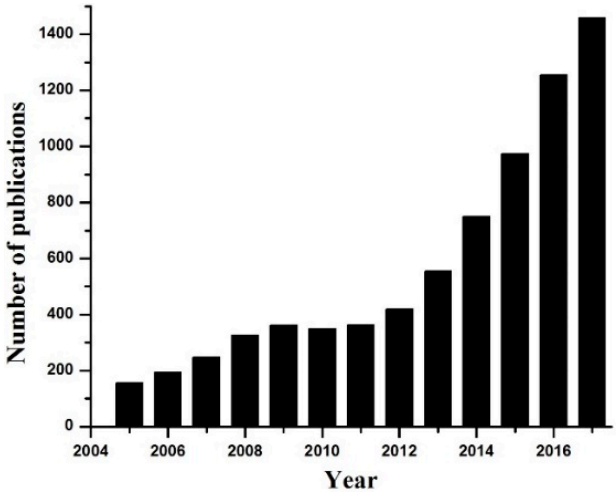


**Figure 1.** Number of published works according to the Scopus search (keyword "carbon dots").

The size of C-dots is usually controlled by the concentration of reactants, temperature of reaction, time, surfactants, additives, etc. For example, the hydrothermal method was used to prepare highly fluorescent C-dots from orange juice [18], glucose [19], banana juice [20], citric acid [21], etc. To date, the majority of the works report the fabrication of blue emitting C-dots with excitation-dependent emission spectra. However, the emission spectra of C-dots can be tuned by doping with some elements such as nitrogen (N), sulfur (S), phosphorus (P), boron (B), or their combinations [22–26]. It has been shown that doping of C-dots leads to the fluorescence enhancement and shift of emission spectra. For example, fluorescent C-dots with green emission spectra (Figure 2) were reported and employed for sensing and cell imaging [15,27].

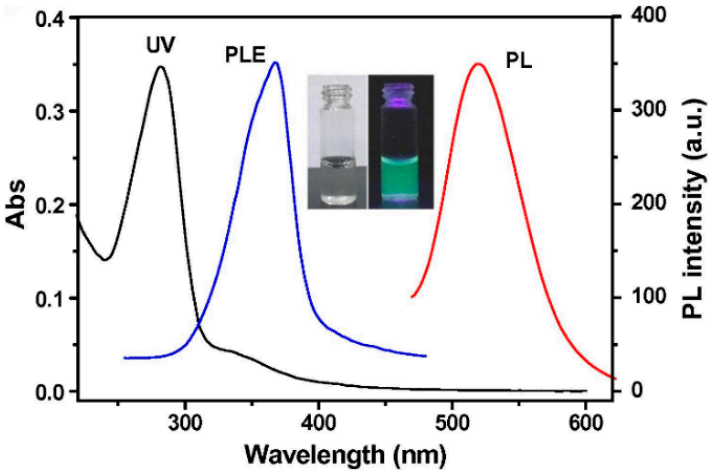


**Figure 2.** UV–vis absorption (UV), PL excitation (PLE), and PL emission (PL) spectra of doped C-dots. Reprinted with permission from reference [15].

C-dots typically show high absorption in the UV range (~287 nm) which can be attributed to n-$\pi^*$ transition of the C=O and $\pi$-$\pi^*$ of the C=C bond. The origin of fluorescence in C-dots was not fully clarified yet, thus, various interpretations can be found in the literature. For example, the origin of fluorescence was attributed to the electron-hole pairs recombination in small $sp^2$ carbon clusters that are localized within a $sp^3$ matrix [28], various surface states and defects [29], surface groups [30], quantum effects (size dependent) and surface passivation [31]. Recently, Wang and coworkers used ultrafast spectroscopy to investigate the origin of green fluorescence in C-dots and graphene quantum

dots [32]. According to their results, the green fluorescence originated from several carbon atoms located on the edge of carbon backbone and some functional groups (carbonyl, carboxyl). Different emission centers and traps can be created with the introduction of dopant atoms into C-dots. As a result, the emission spectra can be tuned to green and even red spectra [33]. However, in some cases dopant elements are located on the surface of C-dots only [34]. Thus, the competition between the optical centers, surface states, and traps is mainly responsible for the emission spectra of doped C-dots. The exact mechanism of fluorescence shifting in doped C-dots still under investigation, thus, further discoveries are expected in near future. Nevertheless, the fluorescent properties of doped C-dots were already utilized for numerous technological applications [2,10,35]. Therefore, the practical usage of doped C-dots for biomedical and sensing applications will be discussed in the following sections.

## 3. Doped C-Dots for Sensing Applications

Analysis of the fluorescent properties of doped C-dots were widely employed for the detection of metal ions, molecules, temperature, pH range, etc. In particular, several research groups utilized doped C-dots for the quantitative detection of the Fe(III) ions [26,36,37]. The fluorescence intensity of doped C-dots decreased monotonically (Figure 3a) as the Fe(III) concentration increased. It was suggested that fluorescence quenching (Figure 3b) occurs due to strong coordination of Fe(III) to the oxygen-rich or amine groups on the surface of doped C-dots.

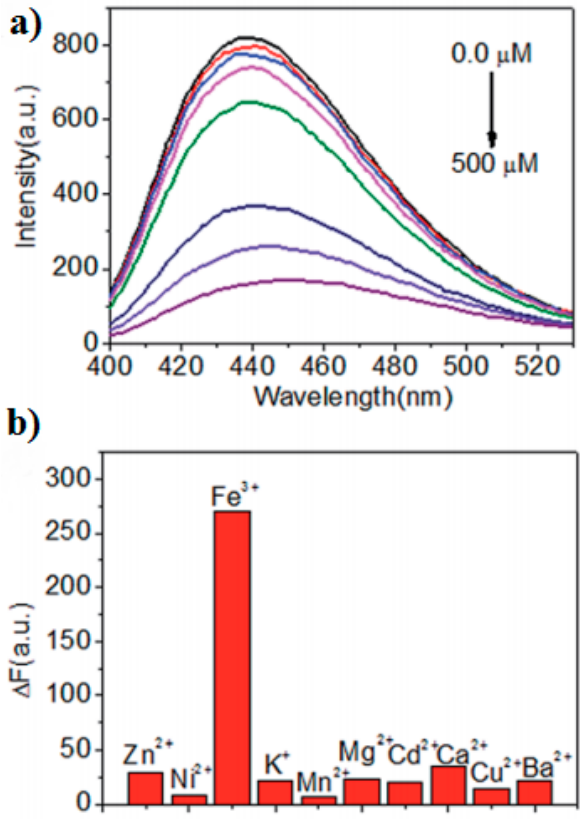


**Figure 3.** (**a**) The emission spectra of sulfur-doped C-dots in the presence of Fe(III) at different concentrations; (**b**) the fluorescence quenching (selectivity) of sulfur-doped C-dots in the presence of different metal ions. Reprinted with permission from reference [26].

It is well-known that the environmental pollution with mercury ($Hg^{2+}$) and lead ($Pb^{2+}$) can raise serious health issues. Recently, doped C-dots were also used as sensors to detect these ions in water. For example, Liu and coworkers reported the preparation of ultrasensitive C-dots for selective detection of $Hg^{2+}$ [38]. Prepared C-dots have been applied for $Hg^{2+}$ detection in tap, lake, and river

water with an excellent detection limit of 1 fM. In another study, authors prepared sensitive $Hg^{2+}$ nanosensor based on nitrogen-doped fluorescent C-dots with a detection limit of 0.23 μM [39]. $Pb^{2+}$ ions were also fluorescently detected by C-dots. For example, C-dots prepared from chocolate have a detection limit of 12.7 nM [40]. Jiang et al. used a microwave method to prepare nitrogen-doped C-dots with a similar detection limit of 15 nM [41]. It was suggested that the quenching mechanism may occur due to the nonradiative electron transfer from the excited states to the electronic orbitals of $Hg^{2+}$ and $Pb^{2+}$. On the other hand, chelation between $Pb^{2+}$ and hydroxyl groups on the surface of C-dots can be another reason for fluorescence quenching [40]. In addition, fluorescent properties of C-dots were also utilized for detection of other metal ions such as $Ag^{+}$ [42], $Cu^{2+}$ [43], $Zn^{2+}$ [44], and $Cr^{6+}$ [45]. Thus, the selectivity of C-dots to some toxic metal ions can be compromised by the presence of other metal ions. To resolve this issue, one can perform the surface modification of C-dots with some receptors for selective detection of metal ions.

The fluorescent properties of C-dots were also widely utilized for the detection of various molecules. For example, fluorescence quenching of C-dots dispersed in dimethyl sulfoxide (DMSO) was reported with acetone addition with detection limit up to $1{:}10^{-7}$ M ratio (DMSO:acetone) [46]. Shan and coworkers showed that boron-doped C-dots demonstrated an excellent ability to detect the hydrogen peroxide $H_2O_2$ and glucose molecules [47]. In this work, the charge transfer between boron and $H_2O_2$ trigger the fluorescence quenching of C-dots, which allow the quantitative detection of hydrogen peroxide in the range of 0.1 to 1.0 mM (Figure 4). In another study, cyclic voltammetry was employed for sensitive detection of glucose with the help of nitrogen-doped C-dots with a detection range of 1–12 mM [48]. Furthermore, nitrogen-doped C-dots were commonly utilized for fluorescent detection of pyridine [49], dopamine [50], amoxicillin [51], microRNA [52], catechol [53], pH and temperature [54], etc. Taking into account such a diverse range of doped C-dots applications, future studies should concentrate on the following open issues: (a) the origin of fluorescence shifting in doped C-dots; (b) the precise localization of doped elements in C-dots; and (c) the role of doped elements in fluorescence sensing.

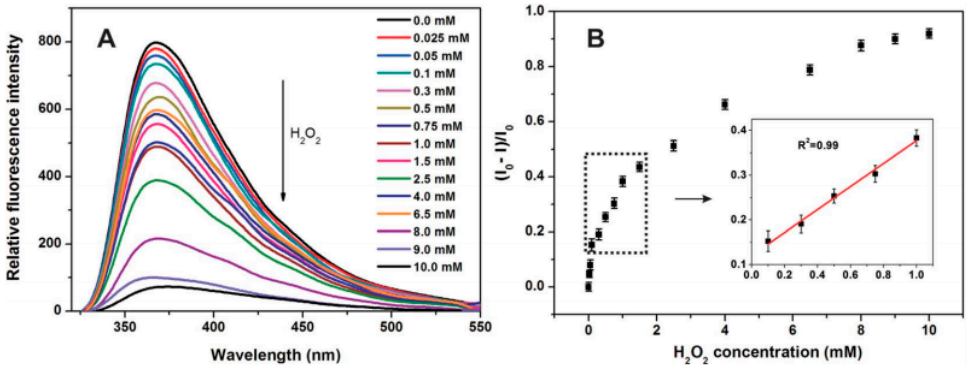


**Figure 4.** (**A**) The emission spectra of boron-doped C-dots in the presence of $H_2O_2$ at different concentrations; (**B**) the fluorescence response of boron-doped C-dots to the $H_2O_2$ at different concentrations. Reprinted with permission from reference [47].

## 4. Doped C-Dots for Biomedical Applications

Compared to conventional organic dyes, C-dots are not suffering from photobleaching and photodegradation. Therefore, C-dots demonstrated a great potential for cell imaging and labeling as a biocompatible fluorescent nanomaterial. For example, numerous studies reported the cell imaging potentials of doped C-dots [55–57]. Due to excitation-dependent fluorescence emission, C-dots can be used as a multicolor nanoprobe that can be excited with different excitation wavelengths. Zhai and coworkers showed that C-dots incubated with L929 cells (Figure 5) could emit blue, green, and red fluorescence upon 405, 488, and 543 nm excitation, respectively [58].

As it was demonstrated by several studies, the fluorescent properties of C-dots can be also efficiently applied for in vivo imaging [59,60]. Excitation-dependent C-dots were injected into a mouse and fluorescent images were collected at different excitation wavelengths (Figure 6). It was found that longer wavelengths (595 nm and beyond) demonstrated better signal-to-background contrast.

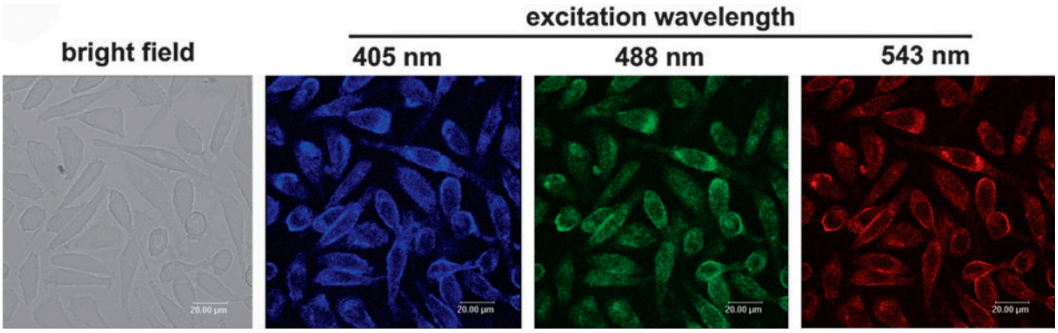


**Figure 5.** Confocal microscopy images of L929 cells incubated with C-dots under different excitation wavelengths. Reprinted with permission from reference [58].

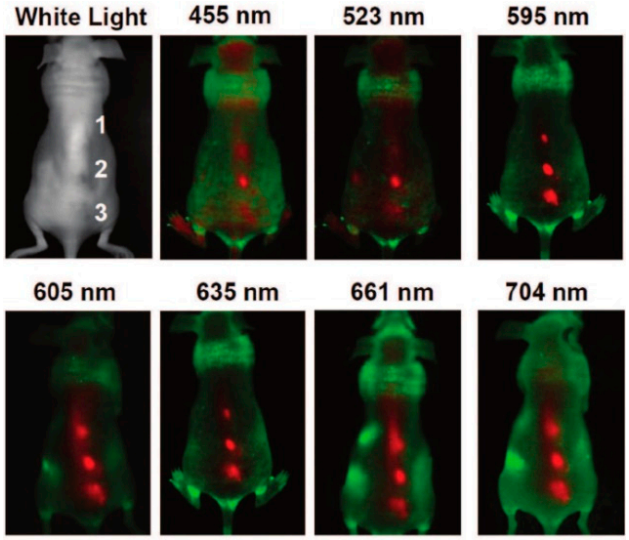


**Figure 6.** In vivo fluorescence images of C-dots injected into nude mouse. Reprinted with permission from reference [60].

Recently, enormous attention has been paid to multifunctional nanoprobes that combine several imaging modalities. In this regard, one can create thin carbon layer coating on the surface of paramagnetic nanoparticles such as $Gd_2O_3$ [61]. Obtained core-shell nanostructure has a longitudinal relaxivity of $r_1 = 4.23 \pm 0.13$ $mM^{-1}$ $s^{-1}$ which is suitable for $T_1$-weighted MRI. At the same, C@$Gd_2O_3$ core–shell nanostructure was also useful for optical imaging of L929 cells thanks to the fluorescent properties of the thin carbon layer. In addition, carbon thin coating can be useful as a protective layer to prevent the leaching of Gd ions into a surrounding environment. On the other hand, paramagnetic metals can be also directly doped into C-dots during the synthesis process. Paramagnetic gadolinium (Gd)-based complexes are widely used as 'positive' $T_1$-weighted contrast agents in radiology [62,63]. Therefore, Gd-doped C-dots were studied extensively for both magnetic resonance imaging (MRI) and cellular imaging.

Chen and coworkers prepared Gd-doped C-dots by the direct calcination of gadopentetic acid (Gd-DTPA) in the air [64]. It was found that prepared Gd-doped C-dots exhibited excellent fluorescence quantum yield ~19.7%. Furthermore, these Gd-doped C-dots have high longitudinal relaxivity

$r_1$ = 5.88 $mM^{-1}$ $s^{-1}$ at 7 T, much higher than commercially available Gd-DTPA ($r_1$ = 3.10 $mM^{-1}s^{-1}$) under the same conditions. Xu and coworkers used a facile hydrothermal method to prepare Gd-doped C-dots with longitudinal relaxivity $r_1$ = 7.36 $mM^{-1}$ $s^{-1}$ at 1.2 T [65]. The imaging site becomes brighter with increasing of Gd concentration (Figure 7), and it obviously highlights that Gd-doped C-dots can be utilized as 'positive' MRI contrast agents. Wang and coworkers used paramagnetic manganese Mn ions as a cheaper and less toxic alternative to Gd(III) [66]. According to results, Mn-doped C-dots have the longitudinal relaxivity of $r_1$ = 7.28 $mM^{-1}$ $s^{-1}$ at 1.2 T, which is comparable to Gd-doped C-dots.

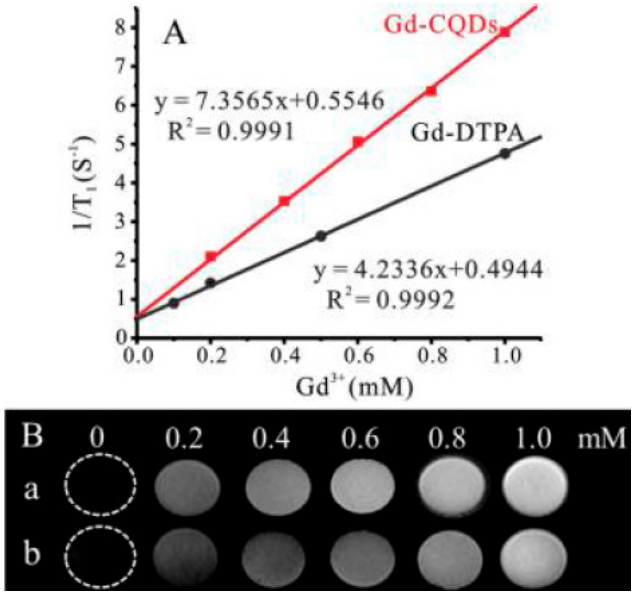


**Figure 7.** (**A**) $T_1$-weighted relaxivity rates of Gd-doped C-dots and Gd-DTPA as a function of $Gd^{3+}$ concentration; (**B**) MRI images of (a) Gd-doped C-dots; and (b) C-Gd-DTPA taken at different concentrations. Reprinted with permission from reference [65].

## 5. Summary and Future Outlook

Doped C-dots can be a versatile material for future biomedical and sensing applications thanks to the unique fluorescent properties, excellent biocompatibility, and high aqueous stability. The fabrication procedure of doped C-dots is quite simple and low-cost due to the wide selection of cheap carbon-rich sources. Furthermore, some fabrication procedures allow the preparation of doped C-dots at relatively large amounts, typically at gram-scale. On the other hand, some issues such as the exact origin of fluorescence, the role of dopant ions, and their location in C-dots were not resolved yet. Thus, these issues should be addressed for fundamental understanding and control of the fluorescence in doped C-dots. One can consider the surface-functionalization of doped C-dots for specificity and selectivity for sensing and biomedical research. For example, C-dots conjugated with folic acid (FA) were able to distinguish the cancer cells from normal cells in a model mixture of cells thanks to a specific interaction between the FA and folate receptor molecule [67]. In a similar manner, doped C-dots can be surface-functionalized for selective recognition of specific ions, molecules, or even cells. The formation of mesoporous surface-functionalized C-dots that can be potentially used in controlled drug delivery can be also another breakthrough in this research area. The existence of limited studies on the development of doped C-dots for $T_2$-weighted MRI ('negative' contrast agents) can be also considered as another unresolved problem. In particular, Dy and Ho ions with high magnetic moments can be introduced into C-dots to prepare 'negative' contrast agents for MRI and optical imaging [68,69]. As one can see, doped C-dots can be a cheap and promising material for various applications such as optics, sensors, biomedicine, energy, etc. Therefore, we strongly believe that the number of studies on doped C-dots will continue to grow in future.

**Author Contributions:** Writing & Editing was performed by T.S.A.

**Funding:** This work was supported by the Social Policy grant provided by Nazarbayev University.

**Conflicts of Interest:** The author declare no conflict of interest.

## References

1. Wang, Y.; Hu, A. Carbon quantum dots: Synthesis, properties and applications. *J. Mater. Chem. C* **2014**, *2*, 6921–6939. [CrossRef]
2. Zhang, J.; Yu, S.H. Carbon dots: Large-scale synthesis, sensing and bioimaging. *Mater. Today* **2016**, *19*, 382–393. [CrossRef]
3. Hou, Y.; Lu, Q.; Deng, J.; Li, H.; Zhang, Y. One-pot electrochemical synthesis of functionalized fluorescent carbon dots and their selective sensing for mercury ion. *Anal. Chim. Acta* **2015**, *866*, 69–74. [CrossRef] [PubMed]
4. Dong, Y.; Cai, J.; You, X.; Chi, Y. Sensing applications of luminescent carbon based dots. *Analyst* **2015**, *140*, 7468–7486. [CrossRef] [PubMed]
5. Du, F.; Zhang, M.; Gong, A.; Tan, Y.; Miao, J.; Gong, Y.; Zou, S.; Zhang, L.; Zhang, L.; Wu, C.; et al. Engineered gadolinium-doped carbon dots for magnetic resonance imaging-guided radiotherapy of tumors. *Biomaterials* **2017**, *121*, 109–120. [CrossRef] [PubMed]
6. Liao, H.; Wang, Z.; Chen, S.; Wu, H.; Ma, X.; Tan, M. One-pot synthesis of gadolinium(III) doped carbon dots for fluorescence/magnetic resonance bimodal imaging. *RSC Adv.* **2015**, *5*, 66575–66581. [CrossRef]
7. Ren, X.Y.; Yuan, X.X.; Wang, Y.P.; Liu, C.L.; Qin, Y.; Guo, L.P.; Liu, L.H. Facile preparation of $Gd^{3+}$ doped carbon quantum dots: Photoluminescence materials with magnetic resonance response as magnetic resonance/fluorescence bimodal probes. *Opt. Mater.* **2016**, *57*, 56–62. [CrossRef]
8. Hutton, G.A.M.; Martindale, B.C.M.; Reisner, E. Carbon dots as photosensitisers for solar-driven catalysis. *Chem. Soc. Rev.* **2017**, *46*, 6111–6123. [CrossRef] [PubMed]
9. Li, H.; He, X.; Kang, Z.; Huang, H.; Liu, Y.; Liu, J.; Lian, S.; Tsang, C.H.A.; Yang, X.; Lee, S.T. Water-soluble fluorescent carbon quantum dots and photocatalyst design. *Angew. Chem. Int. Ed.* **2010**, *49*, 4430–4434. [CrossRef] [PubMed]
10. Zhou, Y.; Benetti, D.; Tong, X.; Jin, L.; Wang, Z.M.; Ma, D.; Zhao, H.; Rosei, F. Colloidal carbon dots based highly stable luminescent solar concentrators. *Nano Energy* **2018**, *44*, 378–387. [CrossRef]
11. Li, X.; Rui, M.; Song, J.; Shen, Z.; Zeng, H. Carbon and Graphene Quantum Dots for Optoelectronic and Energy Devices: A Review. *Adv. Funct. Mater.* **2015**, *25*, 4929–4947. [CrossRef]
12. Peng, H.; Travas-Sejdic, J. Simple aqueous solution route to luminescent carbogenic dots from carbohydrates. *Chem. Mater.* **2009**, *21*, 5563–5565. [CrossRef]
13. Deng, J.; Lu, Q.; Mi, N.; Li, H.; Liu, M.; Xu, M.; Tan, L.; Xie, Q.; Zhang, Y.; Yao, S. Electrochemical synthesis of carbon nanodots directly from alcohols. *Chem. A Eur. J.* **2014**, *20*, 4993–4999. [CrossRef] [PubMed]
14. Hu, S.; Liu, J.; Yang, J.; Wang, Y.; Cao, S. Laser synthesis and size tailor of carbon quantum dots. *J. Nanopart. Res.* **2011**, *13*, 7247–7252. [CrossRef]
15. Liu, Y.; Xiao, N.; Gong, N.; Wang, H.; Shi, X.; Gu, W.; Ye, L. One-step microwave-assisted polyol synthesis of green luminescent carbon dots as optical nanoprobes. *Carbon N. Y.* **2014**, *68*, 258–264. [CrossRef]
16. Yang, Z.-C.; Wang, M.; Yong, A.M.; Wong, S.Y.; Zhang, X.-H.; Tan, H.; Chang, A.Y.; Li, X.; Wang, J. Intrinsically fluorescent carbon dots with tunable emission derived from hydrothermal treatment of glucose in the presence of monopotassium phosphate. *Chem. Commun.* **2011**, *47*, 11615–11617. [CrossRef] [PubMed]
17. Mitra, S.; Chandra, S.; Pathan, S.H.; Sikdar, N.; Pramanik, P.; Goswami, A. Room temperature and solvothermal green synthesis of self passivated carbon quantum dots. *RSC Adv.* **2013**, *3*, 3189–3193. [CrossRef]
18. Sahu, S.; Behera, B.; Maiti, T.K.; Mohapatra, S. Simple one-step synthesis of highly luminescent carbon dots from orange juice: Application as excellent bio-imaging agents. *Chem. Commun.* **2012**, *48*, 8835–8837. [CrossRef] [PubMed]
19. Atabaev, S. Size-tunable carbon nanoparticles with excitation-independent fluorescent properties. *Mater. Today Proc.* **2017**, *4*, 4896–4899. [CrossRef]
20. De, B.; Karak, N. A green and facile approach for the synthesis of water soluble fluorescent carbon dots from banana juice. *RSC Adv.* **2013**, *3*, 8286–8290. [CrossRef]

21. Zhou, M.; Zhou, Z.; Gong, A.; Zhang, Y.; Li, Q. Synthesis of highly photoluminescent carbon dots via citric acid and Tris for iron(III) ions sensors and bioimaging. *Talanta* **2015**, *143*, 107–113. [CrossRef] [PubMed]
22. Zhou, J.; Shan, X.; Ma, J.; Gu, Y.; Qian, Z.; Chen, J.; Feng, H. Facile synthesis of P-doped carbon quantum dots with highly efficient photoluminescence. *RSC Adv.* **2014**, *4*, 5465–5468. [CrossRef]
23. Dong, Y.; Pang, H.; Yang, H.B.; Guo, C.; Shao, J.; Chi, Y.; Li, C.M.; Yu, T. Carbon-based dots co-doped with nitrogen and sulfur for high quantum yield and excitation-independent emission. *Angew. Chem. Int. Ed.* **2013**, *52*, 7800–7804. [CrossRef] [PubMed]
24. Bourlinos, A.B.; Trivizas, G.; Karakassides, M.A.; Baikousi, M.; Kouloumpis, A.; Gournis, D.; Bakandritsos, A.; Hola, K.; Kozak, O.; Zboril, R.; et al. Green and simple route toward boron doped carbon dots with significantly enhanced non-linear optical properties. *Carbon* **2015**, *83*, 173–179. [CrossRef]
25. Barman, M.K.; Jana, B.; Bhattacharyya, S.; Patra, A. Photophysical Properties of Doped Carbon Dots (N, P, and B) and Their Influence on Electron/Hole Transfer in Carbon Dots—Nickel (II) Phthalocyanine Conjugates. *J. Phys. Chem. C* **2014**, *118*, 20034–20041. [CrossRef]
26. Xu, Q.; Pu, P.; Zhao, J.; Dong, C.; Gao, C.; Chen, Y.; Chen, J.; Liu, Y.; Zhou, H. Preparation of highly photoluminescent sulfur-doped carbon dots for Fe(III) detection. *J. Mater. Chem. A* **2015**, *3*, 542–546. [CrossRef]
27. Zhang, J.; Zhao, X.; Xian, M.; Dong, C.; Shuang, S. Folic acid-conjugated green luminescent carbon dots as a nanoprobe for identifying folate receptor-positive cancer cells. *Talanta* **2018**, *183*, 39–47. [CrossRef] [PubMed]
28. Srivastava, S.; Gajbhiye, N.S. Carbogenic nanodots: Photoluminescence and room-temperature ferromagnetism. *Chem. Phys. Chem.* **2011**, *12*, 2624–2632. [CrossRef] [PubMed]
29. Hu, S.-L.; Niu, K.-Y.; Sun, J.; Yang, J.; Zhao, N.-Q.; Du, X.-W. One-step synthesis of fluorescent carbon nanoparticles by laser irradiation. *J. Mater. Chem.* **2009**, *19*, 484–488. [CrossRef]
30. Fang, Y.; Guo, S.; Li, D.; Zhu, C.; Ren, W.; Dong, S.; Wang, E. Easy synthesis and imaging applications of cross-linked green fluorescent hollow carbon nanoparticles. *ACS Nano* **2012**, *6*, 400–409. [CrossRef] [PubMed]
31. Baker, S.N.; Baker, G.A. Luminescent carbon nanodots: Emergent nanolights. *Angew. Chem. Int. Ed.* **2010**, *49*, 6726–6744. [CrossRef] [PubMed]
32. Wang, L.; Zhu, S.J.; Wang, H.Y.; Qu, S.N.; Zhang, Y.L.; Zhang, J.H.; Chen, Q.D.; Xu, H.L.; Han, W.; Yang, B.; et al. Common origin of green luminescence in carbon nanodots and graphene quantum dots. *ACS Nano* **2014**, *8*, 2541–2547. [CrossRef] [PubMed]
33. Sun, Y.P.; Zhou, B.; Lin, Y.; Wang, W.; Fernando, K.A.S.; Pathak, P.; Meziani, M.J.; Harruff, B.A.; Wang, X.; Wang, H.; et al. Quantum-sized carbon dots for bright and colorful photoluminescence. *J. Am. Chem. Soc.* **2006**, *128*, 7756–7757. [CrossRef] [PubMed]
34. Du, Y.; Guo, S. Chemically doped fluorescent carbon and graphene quantum dots for bioimaging, sensor, catalytic and photoelectronic applications. *Nanoscale* **2016**, *8*, 2532–2543. [CrossRef] [PubMed]
35. Hola, K.; Zhang, Y.; Wang, Y.; Giannelis, E.P.; Zboril, R.; Rogach, A.L. Carbon dots—Emerging light emitters for bioimaging, cancer therapy and optoelectronics. *Nano Today* **2014**, *9*, 590–603. [CrossRef]
36. Gong, X.; Lu, W.; Paau, M.C.; Hu, Q.; Wu, X.; Shuang, S.; Dong, C.; Choi, M.M.F. Facile synthesis of nitrogen-doped carbon dots for $Fe^{3+}$ sensing and cellular imaging. *Anal. Chim. Acta* **2015**, *861*, 74–84. [CrossRef] [PubMed]
37. Chen, Y.; Wu, Y.; Weng, B.; Wang, B.; Li, C. Facile synthesis of nitrogen and sulfur co-doped carbon dots and application for Fe(III) ions detection and cell imaging. *Sens. Actuators B Chem.* **2016**, *223*, 689–696. [CrossRef]
38. Liu, R.; Li, H.; Kong, W.; Liu, J.; Liu, Y.; Tong, C.; Zhang, X.; Kang, Z. Ultra-sensitive and selective $Hg^{2+}$ detection based on fluorescent carbon dots. *Mater. Res. Bull.* **2013**, *48*, 2529–2534. [CrossRef]
39. Zhang, R.; Chen, W. Nitrogen-doped carbon quantum dots: Facile synthesis and application as a "turn-off" fluorescent probe for detection of $Hg^{2+}$ ions. *Biosens. Bioelectron.* **2013**, *55*, 83–90. [CrossRef] [PubMed]
40. Liu, Y.; Zhou, Q.; Li, J.; Lei, M.; Yan, X. Selective and sensitive chemosensor for lead ions using fluorescent carbon dots prepared from chocolate by one-step hydrothermal method. *Sens. Actuators B Chem.* **2016**, *237*, 597–604. [CrossRef]
41. Jiang, Y.; Wang, Y.; Meng, F.; Wang, B.; Cheng, Y.; Zhu, C. N-doped carbon dots synthesized by rapid microwave irradiation as highly fluorescent probes for $Pb^{2+}$ detection. *New J. Chem.* **2015**, *39*, 3357–3360. [CrossRef]

42. Gao, X.; Lu, Y.; Zhang, R.; He, S.; Ju, J.; Liu, M.; Li, L.; Chen, W. One-pot synthesis of carbon nanodots for fluorescence turn-on detection of $Ag^+$ based on the $Ag^+$-induced enhancement of fluorescence. *J. Mater. Chem. C* **2015**, *3*, 2302–2309. [CrossRef]
43. Dong, Y.; Wang, R.; Li, G.; Chen, C.; Chi, Y.; Chen, G. Polyamine-functionalized carbon quantum dots as fluorescent probes for selective and sensitive detection of copper ions. *Anal. Chem.* **2012**, *84*, 6220–6224. [CrossRef] [PubMed]
44. Yang, M.; Kong, W.; Li, H.; Liu, J.; Huang, H.; Liu, Y.; Kang, Z. Fluorescent carbon dots for sensitive determination and intracellular imaging of zinc(II) ion. *Microchim. Acta* **2015**, *182*, 2443–2450. [CrossRef]
45. Zhang, H.Y.; Wang, Y.; Xiao, S.; Wang, H.; Wang, J.H.; Feng, L. Rapid detection of Cr(VI) ions based on cobalt(II)-doped carbon dots. *Biosens. Bioelectron.* **2017**, *87*, 46–52. [CrossRef] [PubMed]
46. Jana, J.; Ganguly, M.; Das, B.; Dhara, S.; Negishi, Y.; Pal, T. One pot synthesis of intriguing fluorescent carbon dots for sensing and live cell imaging. *Talanta* **2016**, *150*, 253–264. [CrossRef] [PubMed]
47. Shan, X.; Chai, L.; Ma, J.; Qian, Z.; Chen, J.; Feng, H. B-doped carbon quantum dots as a sensitive fluorescence probe for hydrogen peroxide and glucose detection. *Analyst* **2014**, *139*, 2322–2325. [CrossRef] [PubMed]
48. Ji, H.; Zhou, F.; Gu, J.; Shu, C.; Xi, K.; Jia, X. Nitrogen-doped carbon dots as a new substrate for sensitive glucose determination. *Sensors* **2016**, *16*, 630. [CrossRef] [PubMed]
49. Campos, B.B.; Abellán, C.; Zougagh, M.; Jimenez-Jimenez, J.; Rodríguez-Castellón, E.; Esteves da Silva, J.C.G.; Ríos, A.; Algarra, M. Fluorescent chemosensor for pyridine based on N-doped carbon dots. *J. Colloid Interface Sci.* **2015**, *458*, 209–216. [CrossRef] [PubMed]
50. Jiang, Y.; Wang, B.; Meng, F.; Cheng, Y.; Zhu, C. Microwave-assisted preparation of N-doped carbon dots as a biosensor for electrochemical dopamine detection. *J. Colloid Interface Sci.* **2015**, *452*, 199–202. [CrossRef] [PubMed]
51. Niu, J.; Gao, H. Synthesis and drug detection performance of nitrogen-doped carbon dots. *J. Lumin.* **2014**, *149*, 159–162. [CrossRef]
52. Liu, Q.; Ma, C.; Liu, X.P.; Wei, Y.P.; Mao, C.J.; Zhu, J.J. A novel electrochemiluminescence biosensor for the detection of microRNAs based on a DNA functionalized nitrogen doped carbon quantum dots as signal enhancers. *Biosens. Bioelectron.* **2017**, *92*, 273–279. [CrossRef] [PubMed]
53. Li, H.; Kong, W.; Liu, J.; Liu, N.; Huang, H.; Liu, Y.; Kang, Z. Fluorescent N-doped carbon dots for both cellular imaging and highly-sensitive catechol detection. *Carbon* **2015**, *91*, 66–75. [CrossRef]
54. Song, Z.; Quan, F.; Xu, Y.; Liu, M.; Cui, L.; Liu, J. Multifunctional N,S co-doped carbon quantum dots with pH- and thermo-dependent switchable fluorescent properties and highly selective detection of glutathione. *Carbon* **2016**, *104*, 169–178. [CrossRef]
55. Wang, Y.; Anilkumar, P.; Cao, L.; Liu, J.-H.; Luo, P.G.; Tackett, K.N.; Sahu, S.; Wang, P.; Wang, X.; Sun, Y.-P. Carbon dots of different composition and surface functionalization: Cytotoxicity issues relevant to fluorescence cell imaging. *Exp. Biol. Med.* **2011**, *236*, 1231–1238. [CrossRef] [PubMed]
56. Wang, W.; Li, Y.; Cheng, L.; Cao, Z.; Liu, W. Water-soluble and phosphorus-containing carbon dots with strong green fluorescence for cell labeling. *J. Mater. Chem. B* **2014**, *2*, 46–48. [CrossRef]
57. Zhuo, Y.; Miao, H.; Zhong, D.; Zhu, S.; Yang, X. One-step synthesis of high quantum-yield and excitation-independent emission carbon dots for cell imaging. *Mater. Lett.* **2015**, *139*, 197–200. [CrossRef]
58. Zhai, X.; Zhang, P.; Liu, C.; Bai, T.; Li, W.; Dai, L.; Liu, W. Highly luminescent carbon nanodots by microwave-assisted pyrolysis. *Chem. Commun.* **2012**, *48*, 7955–7957. [CrossRef] [PubMed]
59. Yang, S.T.; Cao, L.; Luo, P.G.; Lu, F.; Wang, X.; Wang, H.; Meziani, M.J.; Liu, Y.; Qi, G.; Sun, Y.P. Carbon dots for optical imaging in vivo. *J. Am. Chem. Soc.* **2009**, *131*, 11308–11309. [CrossRef] [PubMed]
60. Tao, H.; Yang, K.; Ma, Z.; Wan, J.; Zhang, Y.; Kang, Z.; Liu, Z. In vivo NIR fluorescence imaging, biodistribution, and toxicology of photoluminescent carbon dots produced from carbon nanotubes and graphite. *Small* **2012**, *8*, 281–290. [CrossRef] [PubMed]
61. Atabaev, T.S.; Lee, J.H.; Han, D.-W.; Kim, H.-K.; Hwang, Y.-H. Fabrication of carbon coated gadolinia particles for dual-mode magnetic resonance and fluorescence imaging. *J. Adv. Ceram.* **2015**, *4*, 118–122. [CrossRef]
62. Atabaev, T.S.; Lee, J.H.; Han, D.-W.; Choo, K.S.; Jeon, U.B.; Hwang, J.Y.; Yeom, J.A.; Kang, C.; Kim, H.-K.; Hwang, Y.-H. Multicolor nanoprobes based on silica-coated gadolinium oxide nanoparticles with highly reduced toxicity. *RSC Adv.* **2016**, *6*, 19758–19762. [CrossRef]

63. Atabaev, T.S.; Lee, J.H.; Shin, Y.C.; Han, D.-W.; Choo, K.S.; Jeon, U.B.; Hwang, J.Y.; Yeom, J.A.; Kim, H.-K.; Hwang, Y.-H. Eu, Gd-codoped yttria nanoprobes for optical and $T_1$-weighted magnetic resonance imaging. *Nanomaterials* **2017**, *7*, 35. [CrossRef] [PubMed]
64. Chen, H.; Wang, G.D.; Tang, W.; Todd, T.; Zhen, Z.; Tsang, C.; Hekmatyar, K.; Cowger, T.; Hubbard, R.B.; Zhang, W.; et al. Gd-encapsulated carbonaceous dots with efficient renal clearance for magnetic resonance imaging. *Adv. Mater.* **2014**, *26*, 6761–6766. [CrossRef] [PubMed]
65. Xu, Y.; Jia, X.H.; Yin, X.B.; He, X.W.; Zhang, Y.K. Carbon quantum dot stabilized gadolinium nanoprobe prepared via a one-pot hydrothermal approach for magnetic resonance and fluorescence dual-modality bioimaging. *Anal. Chem.* **2014**, *86*, 12122–12129. [CrossRef] [PubMed]
66. Wang, Y.; Wang, T.; Chen, X.; Xu, Y.; Li, H. Mn(II)-coordinated Fluorescent Carbon Dots: Preparation and Discrimination of Organic Solvents. *Opt. Mater.* **2018**, *78*, 118–125. [CrossRef]
67. Song, Y.; Shi, W.; Chen, W.; Li, X.; Ma, H. Fluorescent carbon nanodots conjugated with folic acid for distinguishing folate-receptor-positive cancer cells from normal cells. *J. Mater. Chem.* **2012**, *22*, 12568–12573. [CrossRef]
68. Atabaev, T.S.; Shin, Y.C.; Song, S.-J.; Han, D.-W.; Hong, N.H. Toxicity and $T_2$-weighted magnetic resonance imaging potentials of holmium oxide nanoparticles. *Nanomaterials* **2017**, *7*, 216. [CrossRef] [PubMed]
69. Atbaev, T.S. PEG-coated superparamagnetic dysprosium-doped Fe3O4 nanoparticles for potential MRI imaging. *BioNanoScience* **2018**, *8*, 299–303. [CrossRef]